Earth and Planetary Science Letters 463 (2017) 202–211

Contents lists available at ScienceDirect

Earth and Planetary Science Letters

www.elsevier.com/locate/epsl

Evidence for strong lateral seismic velocity variation in the lower crust and upper mantle beneath the California margin

Voon Hui Lai [a,*], Robert W. Graves [b], Shengji Wei [c], Don Helmberger [a]

[a] Seismological Laboratory, Division of Geological and Planetary Sciences, California Institute of Technology, Pasadena, CA 91125, United States
[b] United States Geological Survey, Pasadena, CA 91106, United States
[c] Earth Observatory of Singapore, 50 Nanyang Ave, 639798, Singapore

ARTICLE INFO

Article history:
Received 19 October 2016
Received in revised form 31 January 2017
Accepted 1 February 2017
Editor: P. Shearer

Keywords:
waveform modeling
lithosphere
California
plate boundary
velocity structure
San Andreas fault

ABSTRACT

Regional seismograms from earthquakes in Northern California show a systematic difference in arrival times across Southern California where long period (30–50 s) SH waves arrive up to 15 s earlier at stations near the coast compared with sites towards the east at similar epicentral distances. We attribute this time difference to heterogeneity of the velocity structure at the crust–mantle interface beneath the California margin. To model these observations, we propose a fast seismic layer, with thickness growing westward from the San Andreas along with a thicker and slower continental crust to the east. Synthetics generated from such a model are able to match the observed timing of SH waveforms better than existing 3D models. The presence of a strong upper mantle buttressed against a weaker crust has a major influence in how the boundary between the Pacific plate and North American plate deforms and may explain the observed asymmetric strain rate across the boundary.

1. Introduction

The lithospheric structure beneath the California margin plays an important role in controlling how the plate boundary between Pacific plate and North American plate deforms. Geodetic studies (Chery, 2008; Schmalzle et al., 2006; Wdowinski et al., 2007) have shown an asymmetry in strain accumulation across the San Andreas Fault (SAF). The asymmetry is attributed to factors including laterally heterogeneous elastic properties in the upper crust (0–20 km) and varying elastic lithospheric thickness across the fault in the lower crust. Here, we present seismic observations that are consistent with the lateral transition in elastic properties across the SAF boundary, involving the lower crust and upper mantle structure beneath the California margin, as shown schematically in Fig. 1.

The seismic lithosphere or lid, as defined in Anderson (1995) is a zone of relatively high seismic velocity in the uppermost mantle, generally overlying a low velocity zone (LVZ) under oceans and cratons. The lid and underlying LVZ are different from the mechanically-defined lithosphere–asthenosphere boundary, although both are closely related, and the seismological layers are often used to outline mechanical structure (Stein and Wysession, 2009). Pure path (1D) models indicate that the Pacific plate has a thick (~60 km) lid overlaying a strong LVZ extending to below a depth of 300 km (Gaherty et al., 1999; Tan and Helmberger, 2007). In contrast, the continental Western United States (WUS) structure is characterized by a relatively slower, thinner lid (10–20 km) along with a weaker mantle LVZ (Grand and Helmberger, 1984). Despite these large lateral differences, the vertical travel times through these two structures are quite similar. Thus, studies utilizing teleseismic phases with nearly vertical ray paths (e.g., most global tomographic models) have diffi-

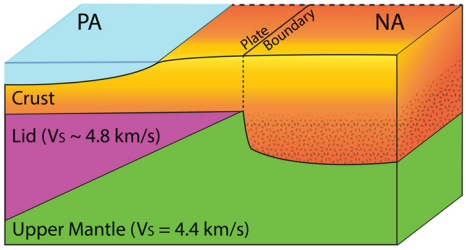

Fig. 1. A schematic drawing of our proposed model. The lid (defined in text), which is faster than its surrounding medium, grows in thickness from the plate boundary towards Pacific plate (PA). In order to better fit the arrival times for inland stations (details in Section 3), the crust below the North American plate (NA) is modeled with a thick, relatively low-velocity crust.

* Corresponding author.
E-mail address: vlai@caltech.edu (V.H. Lai).

http://dx.doi.org/10.1016/j.epsl.2017.02.002
0012-821X/

culty resolving the lateral variation in shear wave velocity structure across the plate boundary.

Using regional S-SS differential travel times, Melbourne and Helmberger (2001) showed that there is lateral variation within the sub-crustal mantle characterized by the presence of a seismic lid beneath California with thickness increasing from 0 km in Eastern California to 55 km along the Pacific plate (see Fig. S1 in Supplementary material (SM)). As the Pacific plate with a thick lid has lower dextral strain compared to the North American plate with a thin lid, they propose that the lid structure may modulate the deformation across the plate boundary. However, the sampling sites of the lid thickness, denoted by the SS reflection points, are located along the coast of Baja California and therefore cannot precisely resolve the lid thickness beneath the main California coastal region.

Understanding how the plate boundary between Pacific plate and North American plate deforms requires an accurate image of the deep structure along the plate boundary. Seismic studies since the 1970s indicate large variability in velocity structure along this boundary. For example, Zandt and Furlong (1982) combined teleseismic travel-time data and thermal models to infer lithospheric-thinning along the San Andreas fault system in northern California. More recently, Wang et al. (2013) used surface wave tomography to map out lateral velocity variations to a depth of 300 km throughout the southwestern United States, finding similar lithospheric thinning to the east of the San Andreas fault in the Mendocino region as well as high velocity regions within the upper mantle at depths up to 200 km that they correlate with fossil slab structures. Other recent studies took advantage of the improved station density coverage to retrieve regional velocity structure of the crust and uppermost mantle using seismic tomography (e.g. Hauksson, 2000; Prindle and Tanimoto, 2006), adjoint waveform tomography (Tape et al., 2009) or receiver function techniques (e.g. Zhu and Kanamori, 2000; Yan and Clayton, 2007; Lekic et al., 2011; Levander and Miller, 2012; Ford et al., 2014). Many of these regional velocity features are incorporated in the development of 3D velocity models by the Southern California Earthquake Center (SCEC), which are discussed later.

Multiple earthquakes, namely the 2014/03/10 Mw 6.8, 2005/06/15 Mw 7.2, and 2010/01/10 M6.5 events in Mendocino region and the 2014/08/25 Mw 6.0 Napa earthquake, present a unique opportunity to directly study the lateral variation in the lower crust–upper mantle structure beneath the California margin using regional waveforms. The earthquakes occurred in Northern California and the waveforms were recorded by the BK network operated by the Northern California Seismic Network (NCSN) and the CI network operated by the Southern California Seismic Network (SCSN) at regional distances (3–11°) (Fig. 2a inset). The recorded waveforms exhibit significant travel time differences (discussed in Section 2), suggesting possible lateral heterogeneity of the lithospheric structure beneath the California margin.

3D waveform-modeling is useful to investigate anomalous behaviors in the seismic wave field, but can be prohibitive when modeling at large continental scales due to high computational cost. One previous known effort in continental-scale modeling is by Ji et al. (2005) which is able to explain large scale Rayleigh-wave multipathing phenomenon across western North America, but lacks resolution for detailed study on ocean–continent transition. Specifically modeling the crustal-sensitive waves that sample the whole continental margin on a reduced regional scale allows us to refine current velocity models and constrain key features across the plate boundary.

In this study, we show that the travel times of the regional SH waveforms from these events cannot be well explained by existing 1D and 3D velocity models, which are poorly constrained in lower crust–upper mantle structure. We propose that a fast seismic layer beneath the California coast coupled with a thick, relative slow crust beneath eastern California is necessary to explain the discrepancies in travel times. The lateral variation of velocity in the lower crust–upper mantle region in our proposed model suggests a similar lateral variation in lithospheric strength which may play a strong role in modulating long term plate deformation and explain the strain rate asymmetry across the SAF.

Table 1
A description of the modified 1-D 'Gil7' model. The main modification is a simplification of the crustal layer where the number of layers is reduced from 7 to 3. The Moho depth in this model is 25 km. The parameters of the fast lid and the thicker, slower crust used in western and eastern parts, respectively, of this study's preferred model, are listed in parentheses.

Layer	Thickness (km)	V_s (km/s)	V_p (km/s)	Density (g/cc)
Upper crust	5	2.60	4.50	2.40
	12	3.40	6.21	2.68
Lower crust	8 (18)	3.98 (3.70)	6.89 (6.70)	3.00 (2.80)
(Lid)	(varies)	(4.80)	(8.30)	(3.20)
Upper mantle	–	4.40	7.80	3.00

2. Observations

The challenge in studying the ocean–continent plate boundary using regional waveforms in California is that it is difficult to model the different types of waveforms (P, SH and SV) simultaneously because of the limited aperture of the station distribution and the nodes in the radiation patterns for strike-slip events. In this study, we concentrate on the tangential component in displacement, because the stations are located close to the maxima of SH wave radiation pattern for the earthquakes we analyze.

We perform cross-correlation to see how the travel times of the observed SH waveforms compare with that computed from a 1-D velocity model (see Table 1) modified from the layered 'Gil7' velocity model (Dreger and Romanowicz, 1994). The 1-D synthetics are computed using frequency-wavenumber method by Zhu and Rivera (2002). The 'Gil7' velocity model is derived from broadband waveform modeling and routinely used in moment tensor inversions in Northern California. The 'Gil7' model is a relatively fast model, which has a shallow Moho boundary at 25 km and includes a fast, mafic lower crust with a P-wave velocity (V_p) of 6.89 km/s and shear wave velocity (V_s) of 3.98 km/s, as revealed from the San Francisco Bay area seismic imaging experiment (BASIX) in 1991 (Brocher et al., 1994). The time differences between the data and synthetics will show how much the 1-D velocity model deviates from the true velocity structure. In this study, we use published moment tensor solutions provided by the ANSS Comprehensive Earthquake Catalog (listed in Table 2). We concentrate our analysis in the period range of 30 to 50 s. The waveforms sample up to a depth of 100 km and are sensitive to both the lower crust and upper mantle structure (see Fig. S2 in SM for sensitivity kernel produced using tools from Herrmann, 2013).

For both Mendocino and Napa earthquakes, the observed long period SH waves show a systematic pattern of later arrival times (positive time delay) for sites in eastern California and early arrival times (negative time delay) for sites along the coast, demonstrating that the velocity structure varies laterally across California (Fig. 3). The range of time shifts for the 2014 Mendocino event is stronger than that seen for the 2014 Napa earthquake, suggesting that the waveforms from the Mendocino event are able to better sample this considerable structural variation, which extends from Mendocino region to the south of Napa region along the coast. Additionally, the pattern and strength of the time shifts seen for the 2014 Mendocino event are consistent with that found for other events of similar magnitudes in the Mendocino Triple Junction

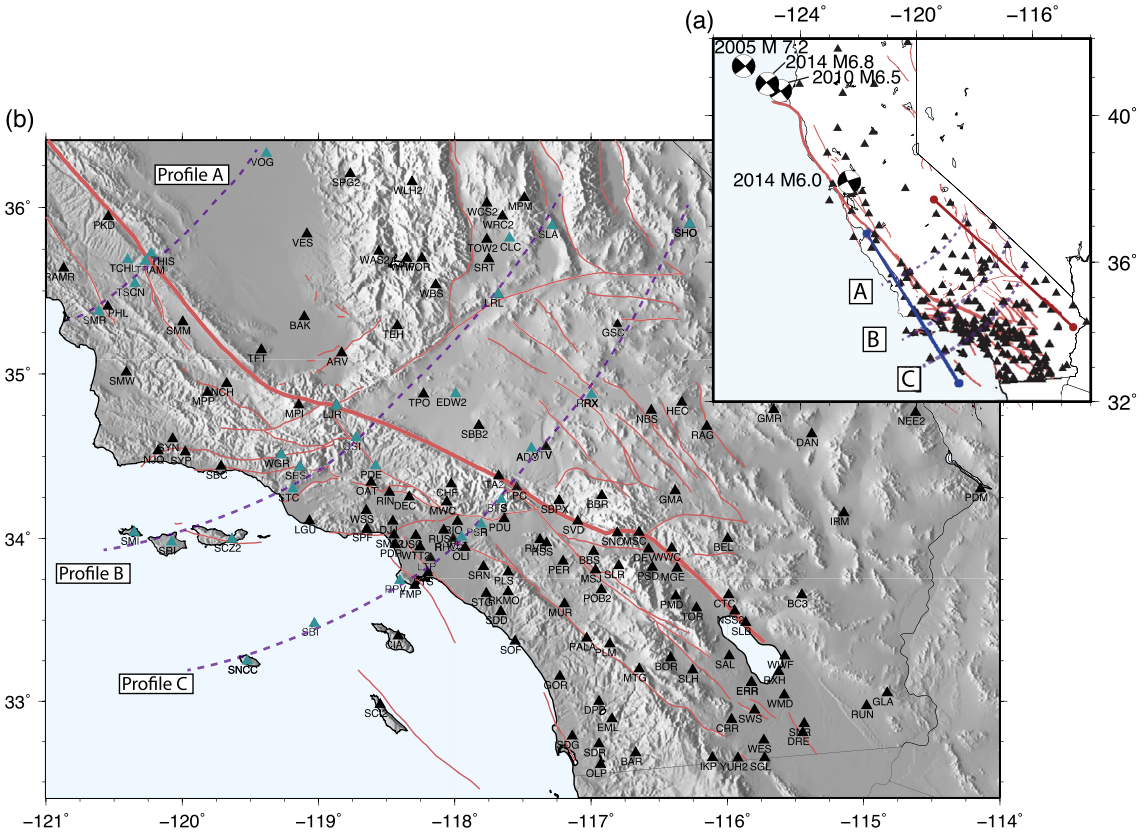

Fig. 2. (a) The inset shows the location of the earthquakes in Mendocino and Napa regions (see Table 2 for details), along with the distribution of broadband stations from NCSN and SCSN used in this study. The blue line displays the location of coastal stations and the red line shows the location of inland stations along radial profiles discussed later. The three azimuthal profiles (Profile A, B and C) marked in purple dashed lines are used to examine the timing and waveform variations as a function of back azimuth to the events. (b) Topographic map zoomed in on the location of SCSN stations and azimuthal profiles featured in this study. The fault map is provided by Jennings (1994) where the San Andreas Fault is highlighted in bold red line. (For interpretation of the colors in this figure, the reader is referred to the web version of this article.)

Table 2
The earthquake source parameters used in this study are provided by the ANSS Comprehensive Earthquake Catalog (ComCat), which can be assessed at http://earthquake.usgs.gov/earthquakes/search/.

Event name	Origin time (UTC)	Moment magnitude (Mw)	Latitude	Longitude	Depth (km)	Focal mechanism		
						Strike	Rake	Dip
2014 Napa	2014–08–24 10:20:44.070	6.0	38.215	−122.312	11.1	155	172	82
2014 Mendocino	2014–03–10 05:18:13.430	6.8	40.829	−125.134	16.6	318	−169	88
2005 Mendocino	2005–06–15 02:50:54.190	7.2	41.292	−125.953	16.0	317	172	83
2010 Mendocino	2010–01–10 00:27:39.320	6.5	40.652	−124.692	29.3	233	0	85

region (Fig. 4). As a check, we also compute our own moment tensor solutions using the cut-and-paste (CAP) inversion method (Zhao and Helmberger, 1994 and Zhu and Helmberger, 1996) and find that the time shift patterns are stable even with small variations in focal mechanisms (see Fig. S3 in SM). This emphasizes the role of lateral velocity variations in controlling the arrival times as opposed to effects related to source location or mechanism.

Aligned waveforms from stations along the coast (blue profile line in Fig. 2a) show Sn-phase moveout of approximately the apparent shear wave velocity, 4.7 km/s (Fig. 5, top panels). However, waveforms from inland stations, along the red profile line in Fig. 2, show slower Sn-phase moveout velocities less than ∼4.7 km/s (Fig. 5, bottom panels). As discussed earlier, this feature is much stronger for the Mendocino event than for the Napa event, and it suggests the presence of a shear wave velocity region along coastal California that is faster than any of the structures depicted in the 'Gil7' model (see Table 1). Note that slight mislocation of the epicenter and origin times only shifts the record sections, leaving the apparent velocity unchanged.

Similarly, we observe in the azimuthal record sections (Fig. 6), which span across a few hundred kilometers, that the Sn waves arrive systematically earlier for coastal and offshore stations relative to the inland sites. In addition, while the arrivals following the direct Sn at the inland stations show large amplitude coherent wave trains, the later arrivals at the coastal stations become less coherent and their amplitudes are significantly decreased. The transition in waveform character described above occurs near the SAF on the northernmost profile (Profile A, see Fig. 2 for location), and then shifts to west of the SAF further south (Profiles B and C).

The difference in travel times suggest that there is a strong east–west lateral variation in the lower crust–upper mantle velocity structure beneath California, where the structure beneath the coastal and offshore stations has a substantially faster shear wave velocity compared to that beneath the inland stations. The variation in velocity structure appears independent of distance, since all three profiles display similar patterns in travel time shift. The heterogeneity in structure may also contribute to the distortion of later arriving waves as seen in the coastal stations.

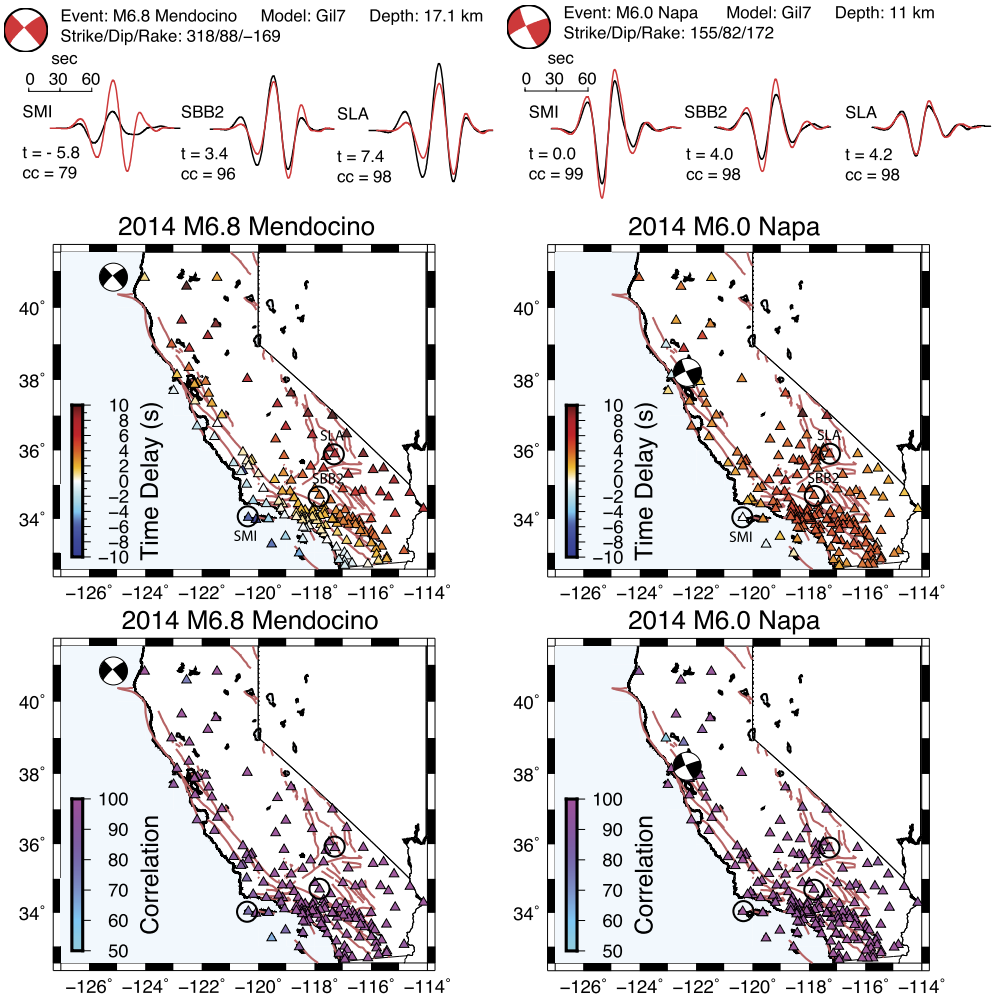

Fig. 3. An example of cross-correlation results shown for three stations, SMI (coastal), SBB2 (near SAF) and SLA (Eastern California), where the time delays and correlation values are stated. Maps show the computed time shifts between the observed long period (30–50 s) SH waves and the 1-D synthetics for both earthquake events. Cooler color indicates the observed waves arrive earlier than predicted by the synthetics and warmer colors indicate later wave arrivals. The average time differences (calculated from the eastern border of California to the coast) are about 7 s (Napa) and 14 s (Mendocino) respectively. The correlation of the observations with synthetics is high, with average coefficient above 0.90. The fit decreases for some coastal stations for the Mendocino event due to waveform interference at later arrival times but does not affect the arrival time of the first peak of the wave train. (For interpretation of the colors in this figure, the reader is referred to the web version of this article.)

3. Modeling

We propose that the systematic, east–west variation in arrival times of the SH waves is due to the variation in the velocity structure in the lower crust–upper mantle along the plate boundary. There are several scenarios that can contribute to the variation, such as different crustal thicknesses, presence of fast seismic lid, and/or different velocity in the lower crust–upper mantle structure. A recent study by Tape et al. (2012) shows that the Moho depth varies from 20 km offshore to 35 km inland across Southern California (along profile C in Fig. 2). However, the difference in arrival times cannot be solely from variation in crustal thickness. A quick calculation from synthetics generated from 1-D velocity models shows that for every increase in crustal thickness of 10 km, the arrival times are delayed by ∼2.5 s (see Fig. S4 in SM). A 14 s time difference (calculated from the east California to the coast) would suggest a 56 km difference in crustal thickness across California, which far exceeds the expected crustal thickness in this region.

Thus, we propose that the early arrival times at the coastal stations are predominantly due to the presence of a seismic lid west of the SAF and parallel to the coast, as presented schematically in Fig. 1. In short, this seismic lid shares the same properties as the one observed within the Pacific plate, with a preferred SH velocity of 4.78 km/s (Tan and Helmberger, 2007). The presence of the lid is consistent with the observed apparent velocities of the long period Sn waveforms recorded by stations along the coast. As the seismic lid is much faster than the upper mantle (V_s of 4.8 km/s compared to 4.4 km/s), it has significant impact in shortening the travel times. The velocity contrast across California was previously observed in a 3-D tomographic study by Hauksson (2000), where he determined a high V_p (8.2 km/s) structure at a depth around 20 km beneath the Southern California coastline. The structure is inferred to have a V_p/V_s ratio of 1.77, which translates to a V_s of 4.6 km/s, slightly lower than our estimated SH velocity of the lid. This difference can possibly be explained by seismic anisotropy in the oceanic plate where Tan and Helmberger (2007) found SH velocity to be about 5% faster than SV velocity. The gradual decrease in travel times with back azimuth suggests that the lid may grow in thickness from inland towards the coast. The lid thickness is less well constrained compared to the crustal thickness, and can be as thick as 60 km, as suggested by Tan and Helmberger (2007).

To explain the delayed arrival times for inland stations, we propose the velocity structure beneath stations east of the SAF is significantly slower than to the west. This is consistent with previous studies that have found eastern California is character-

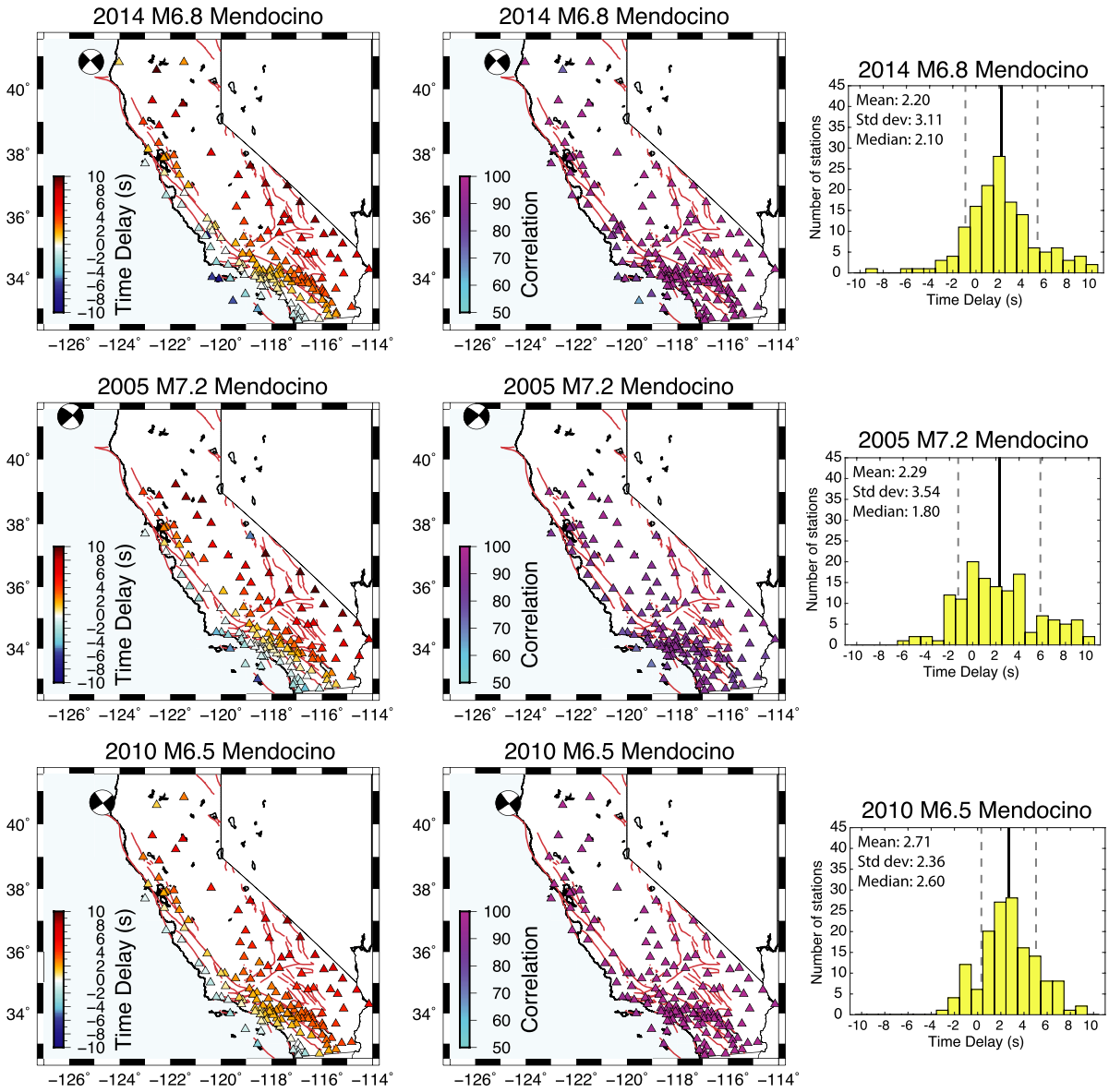

Fig. 4. Similar to Fig. 3, where maps show the time delay between the observed long period SH waves and the 1-D synthetics for three events of similar magnitudes in the Mendocino region. The correlation of the observations with synthetics is high, with average coefficient above 0.90. For stations towards the coast, the observed waves arrive earlier than predicted by the 1-D synthetics, indicated by cooler colors. For stations in eastern California, the observed waves arrive later than predicted by the 1-D synthetics, indicated by warmer colors. Histograms to the right of the maps show the distribution of the time delays for each event. (For interpretation of the colors in this figure, the reader is referred to the web version of this article.)

ized by a relatively thick crust (Zhu and Kanamori, 2000) comprised of relative low seismic velocities especially within the lower crust beneath the Mojave block (Ammon and Zandt, 1993; Helmberger et al., 2001).

Our proposed model, shown in Fig. 7, is a combination of the modified 1-D 'Gil7' velocity model with thicker and slower crust on the east, and a fast lid with a shear wave speed of 4.8 km/s, increasing in thickness from 0 km to 70 km offshore. The velocity structure remains uniform trending northwest-to-southeast as indicated in Fig. 7. The boundary, where the lid grows in thickness, tracks the stations with zero time shifts (from Fig. 3 and Fig. 4) and runs mostly parallel with SAF in Northern California, and shifts to the west by 100 km after the 'Big Bend' in Southern California. The lower crustal velocity at 3.7 km/s in Eastern California is compatible with regional modeling of Basin and Range events (Song et al., 1996).

To test our hypothesis, we use the 3-D finite difference method (Graves, 1996) to generate synthetics from our proposed model. The model is discretized with a uniform spacing of 0.5 km. We consider a 2-step approach to test the effects of the main features in our proposed structure, which are the fast lid on the west, and the low velocity thicker crust on the east. We first model the synthetics using a velocity model that only includes the fast lid, which improves the fit of the SH arrival times between the synthetics and data for the coastal and offshore stations, but does not affect the inland stations (Fig. 8b). We then use the model that includes both the fast lid and the low velocity thicker crust, and this significantly improves the fit for most inland stations (Fig. 8c). However, this model also decreases the fit for stations in the southernmost portion of California, particularly those in the Salton Trough and Imperial Valley region. It is widely known that this region has a relatively thin crust (e.g. Hauksson, 2000 and Tape et al., 2012), which is clearly inconsistent with our proposed "thick crust" model. This indicates that additional 3D complexities beyond that currently included in our simplified representation are required to more fully explain all of the observations. The structural complex-

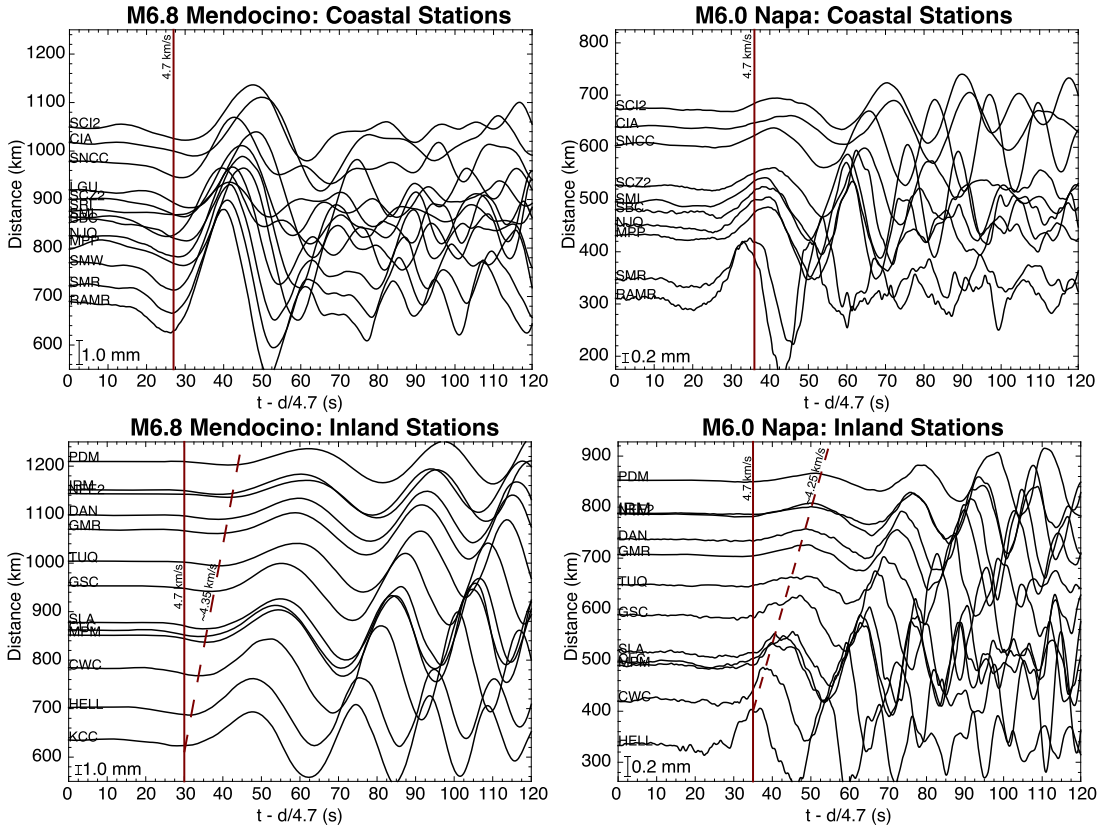

Fig. 5. The record sections display broadband (1–100 s) SH waveforms in displacement from the coastal stations in the top row (west of SAF; blue line in Fig. 2a) and from inland stations in the bottom row (located in Eastern California; indicated by red line in Fig. 2a) for both earthquake events. The arrivals of the first peak, which are the long period Sn waves, are aligned for coastal stations, showing that the waves are traveling at about the apparent shear wave velocity of ∼4.7 km/s. For inland stations, there is a strong move-out of the peaks across distances indicated by the dashed lines, showing the peaks are traveling slower than the reduction velocity (4.7 km/s). The move-out velocities are ∼4.35 km/s and ∼4.25 km/s for the Mendocino and Napa events, respectively.

ities in this southernmost portion of the model should also be considered when performing similar analysis of the reverse profile (south to north) using earthquakes occurring in the Baja California region such as the 2010 M7.2 El Mayor–Cucapah event. Incorporating these modifications is the subject of future work.

We further compare our model with the present 3D velocity models available through the SCEC community (Fig. 9). There are three regional velocity models in total: the USGS Bay Area model v08.3.0 for Northern California (Aagaard et al., 2010) and two southern California Community Velocity Models (CVM), which are CVM-S4.26 (Lee et al., 2014) and CVM-Harvard 15.1.0 (Shaw et al., 2015). The main advantage of the existing 3D velocity models is that they have high resolution on basin and upper crust structure and those structures are well-resolved. The lower crust–upper mantle structure in the 3D models are derived from seismic tomography and teleseismic surface wave data, and they generally have a poorer resolution, compared to the upper crust. To construct a state-wide velocity model for comparison, we utilize the SCEC Unified Community Velocity Model (UCVM 15.10.0) software framework (http://scec.usc.edu/scecpedia/UCVM). This software package allows the combination of the USGS Bay Area model with either of the southern California CVMs. The UCVM package also prescribes a generic 1D velocity model (Hadley and Kanamori, 1977) for regions not described by the 3D velocity models. The boundary for each of the 3D velocity models is shown in Fig. S5 in SM. The slight discontinuities at the boundaries where the different velocity models are combined have no significant impact as the waveforms used in subsequent analysis are filtered at long period (30–50 s).

For the coastal region, our model generally compares well with the UCVM 3D models. Our model shares some key characteristics with these 3D models as illustrated in the shear wave velocity cross-sections shown in Fig. 10. These include: 1) the relatively thin crust (average 15 km) under the coastal region, which is evident in the northern region covered by the USGS Bay Area model, and 2) the presence of fast seismic velocities (up to $V_S = 5.0$ km/s) below the Moho in the southern region, particularly for CVM-S4.26, and to a lesser extent for CVM-H.

For the inland region, both sets of UCVM 3D model synthetics are too fast compared to the data, which is primarily due to the fast (4.0 km/s) structure in the USGS Bay Area model in the lower crust. Hence, our model emphasizes the need for a slower structure beneath Eastern California compared with these models. On the other hand, the UCVM 3D model including CVM-H does well at matching the time delays near Imperial Valley, suggesting this model is adequately capturing the thinning of the crust in this region. The azimuthal record sections for all the models are shown in Fig. S6 in SM. These profiles further highlight the timing differences among the models, and in particular demonstrate that the UCVM 3D models predict arrivals at the inland sites that are up to 15 s earlier than the observations. We also note that the UCVM 3D models have better fits for the amplitude of the later arrivals in the Love wave train, indicating these models have a better-resolved shallow crustal structure than our simplified model.

4. Discussion and conclusion

The simple seismic velocity model we have developed in the present work only includes lateral variations in one horizontal di-

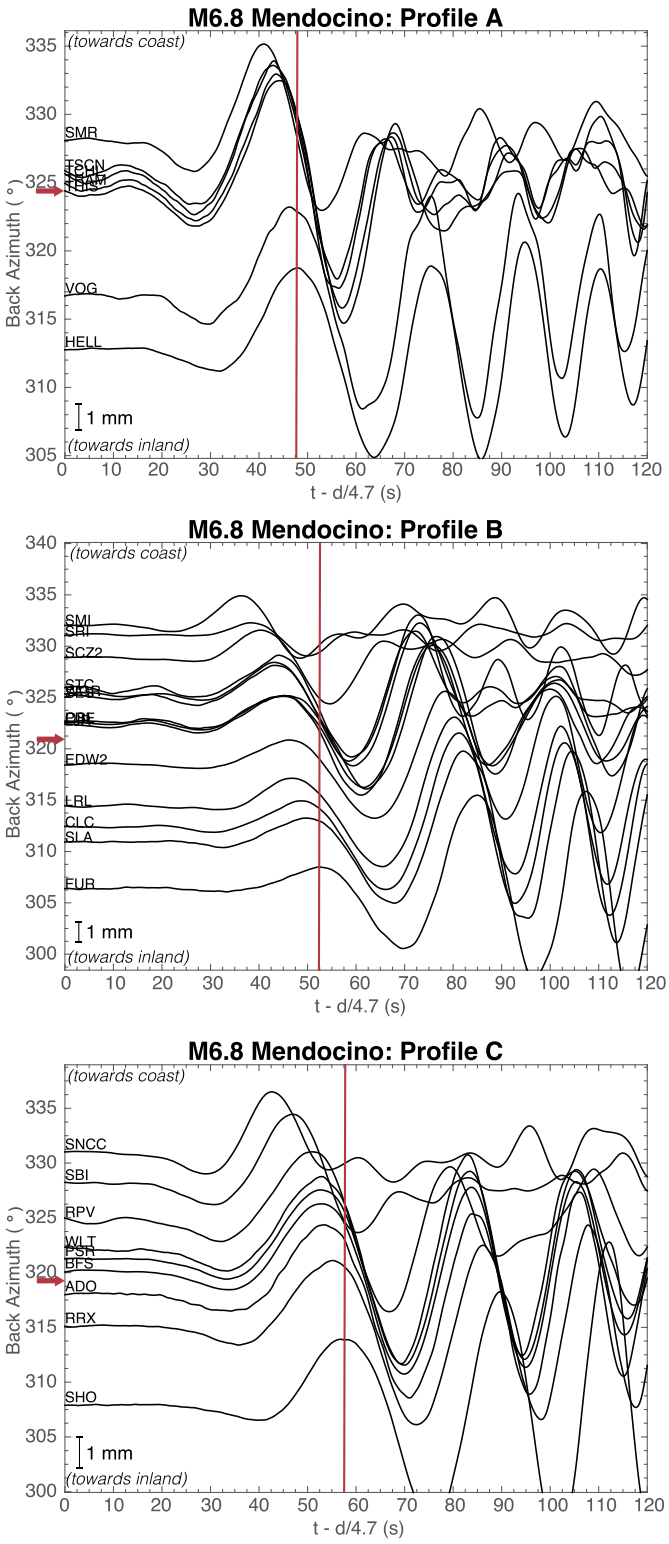

Fig. 6. Figure shows azimuthal record sections of the broadband SH waves from the 2014 Mendocino event, with time plotted using a reduction velocity of 4.7 km/s. The station locations and profile lines are shown in Fig. 2. The back azimuth increases as the station location shifts from inland towards the coast. The red line acts as a guide to show the SH waves arrive earlier for stations towards the coast. The location of SAF with respect to the stations is indicated by the red arrow in each record section. (For interpretation of the references to color in this figure, the reader is referred to the web version of this article.)

mension, and is thus insufficient to capture the full 3D complexity of the velocity structure in California, as illustrated in Fig. 8c. In any case, even though our model is simple, it does provide direct evidence for a key characteristic of the lower crust–upper mantle structure beneath, which is the strong west–east lateral seismic velocity contrast across the plate boundary.

Our work suggests that the fast seismic lid feature extends beyond Baja California as initially proposed by Melbourne and Helmberger (2001) and is, in fact, a continuous feature parallel to the SAF along the California coastline. The waveforms recorded from the Mendocino events propagate south and sample the lower crust–upper mantle structure along the entire region. In addition, the travel time move-out in the observed waveforms is significantly more pronounced for the Mendocino event compared to the Napa event. The Mendocino event originated 80 km offshore, and hence the waveforms sample more of the oceanic lid along the coast. The propagation path of the waveforms from the Napa event, which originated inland, are mostly restricted to inland paths, away from the coastline and therefore the move-out effect due to the lid is less evident.

The absolute thickness of the lid is not well constrained, as the thickness trades off with the lid velocity. However, the general behavior of the lid growing in thickness holds as we see in Fig. 3 and Fig. 4, there is a gradual increase in travel time difference for the waveforms as the ray paths shift westward. In order to the fit the observations, the lid has to be significantly faster (i.e. $V_S = 4.8$ km/s) than the velocity of upper mantle ($V_s = 4.4$–4.5 km/s) in reference models. The high shear wave velocity of the lid suggests a highly mafic composition, consistent with the composition for Pacific oceanic lithosphere (Tan and Helmberger, 2007). The currently available 3D velocity models for California do not adequately capture the travel-time variations seen in these regional waveform data. This suggests that these data could be used as constraints in future updates of these 3D models.

The observed strong lateral variation in the upper mantle structure beneath California likely contributes to the strain rate asymmetry and should play a significant role in modulating plate deformation. Assuming the seismic velocity as a proxy for lithospheric strength, the lid beneath the Pacific plate, with higher velocity, is thus much stronger than its surroundings and lends strength to the Pacific plate. The shear wave velocity of the lid ($V_s = 4.8$ km/s) is significantly higher than its surrounding medium: the lower crust has a maximum V_s of about 4.0 km/s and the upper mantle averages V_s of about 4.4 km/s. On the other hand, the relatively lower velocity of the deep crust and absence of a strong lid beneath the North American plate suggests weaker lithospheric strength. Thus, the upper mantle of the Pacific Plate should deform more rigidly and differs from the North American Plate, which is in the plastic flow regime (Kohlstedt et al., 1995).

Schmalzle et al. (2006) showed a scenario on how variation in effective elastic thickness (EET) can explain the strain rate asymmetry across the San Andreas fault in the Carrizo Plain region in central California. Their best fitting result requires a 38 km EET west of SAF and an average of 12 km EET east of SAF. Taking the interseismic strain rate to be inversely proportional to the effective elastic thickness (EET) of the lithospheric plate, Chery (2008) further showed that the interseismic strain rate profiles across northern, central and southernmost California are best modeled with a thin EET along the plate boundary and thick EET on the Pacific plate and Sierra Nevada province. The change in EET across the plate boundary follows closely along the SAF trace in northern and central California, and moves ~75 km westward towards Elsinore Fault in southernmost California (see Fig. S7 in SM). Similarly, from geodetic data inversion for slip rates on faults in California, Platt and Becker (2010) proposed that (1) the present velocity field reflects long-term plate motion and (2) the real lithospheric trans-

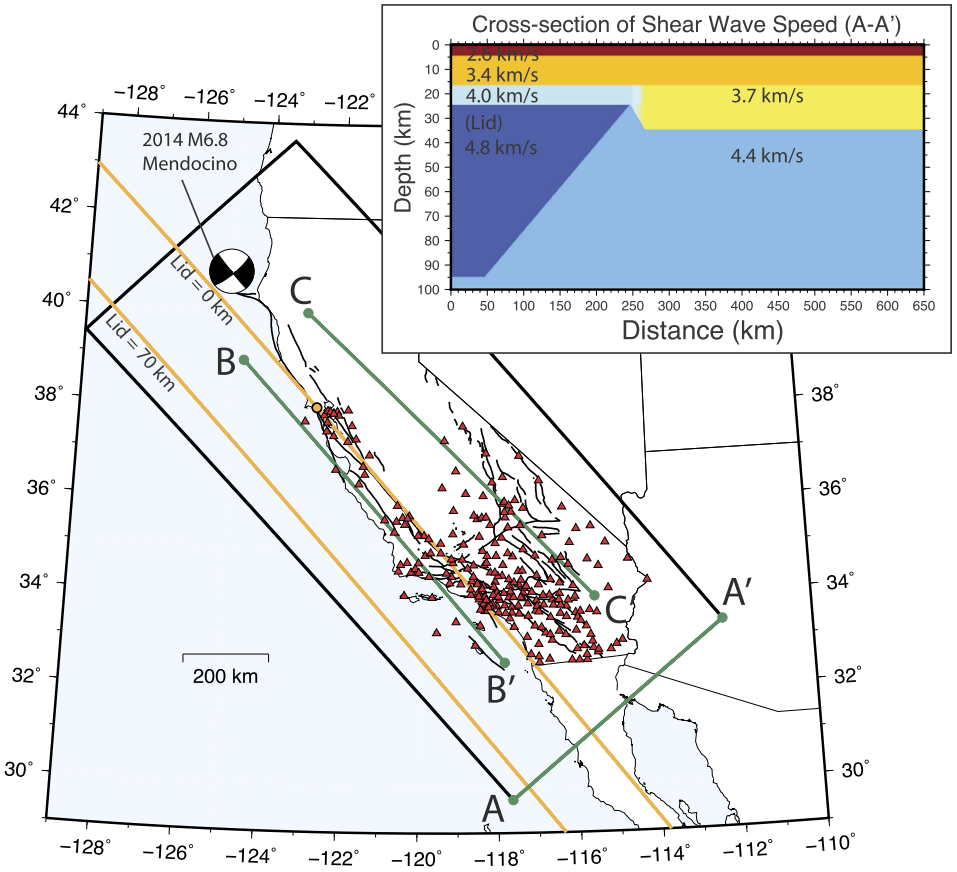

Fig. 7. Map illustrates the configuration used in the 3-D finite difference modeling. Black box marks the surface boundary of the 3-D grid. The cross section profile (A–A′) shows the 2-D shear wave velocity structure, which is a modification of the 1-D 'Gil7' model (see Table 1) with the lid structure, the thicker crust on the east and an additional low velocity zone. Yellow parallel lines delineate the zone where the lid thickness increases from 0 to 70 km. The event modeled is the 2014 M 6.8 Mendocino earthquake. Profile B–B′ and Profile C–C′ are shown in Fig. 10. (For interpretation of the colors in this figure, the reader is referred to the web version of this article.)

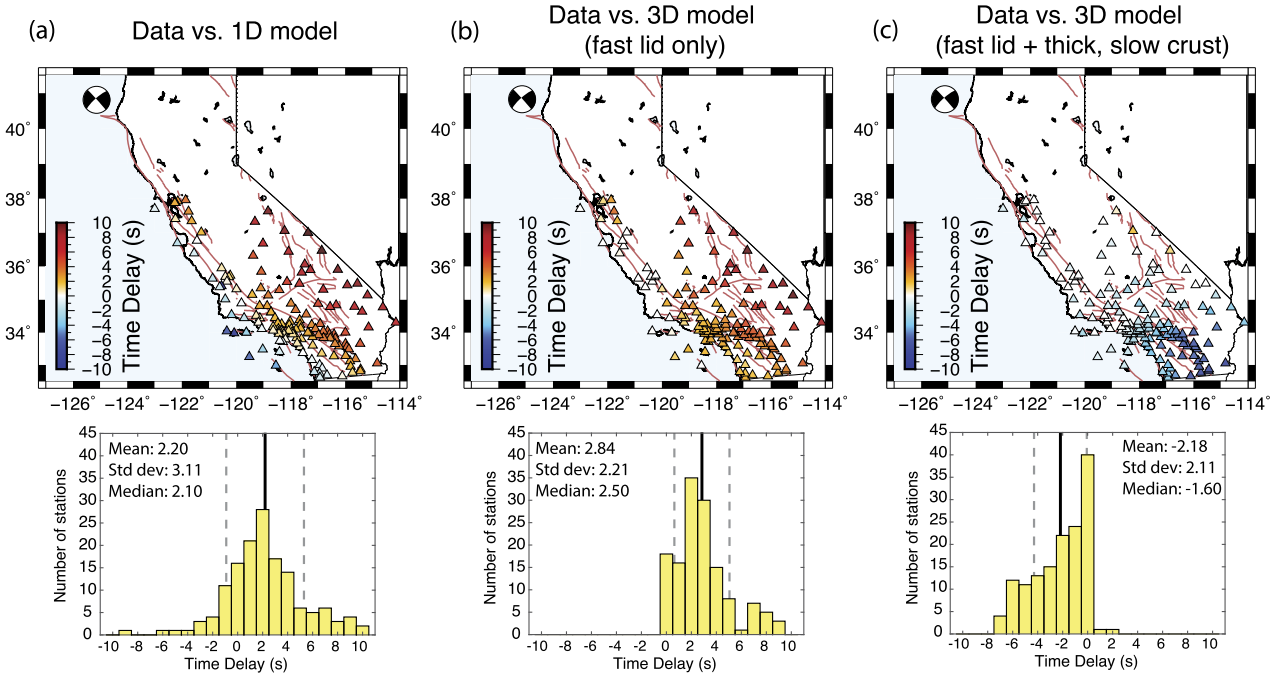

Fig. 8. Maps show the time delay between the long period SH waves from the 2014 Mendocino event, and (a) the 1-D synthetics from 'Gil 7' model (same as Figs. 3, 4), (b) the 3-D synthetics from our proposed model with the lid only (no thick crust on the east), and (c) model with inclusion of both the lid and thicker, slower crust on the east. The histogram of the time shifts for each model comparison are shown below the map. Cooler color indicates the recorded seismograms arrive earlier than the synthetics. (For interpretation of the colors in this figure, the reader is referred to the web version of this article.)

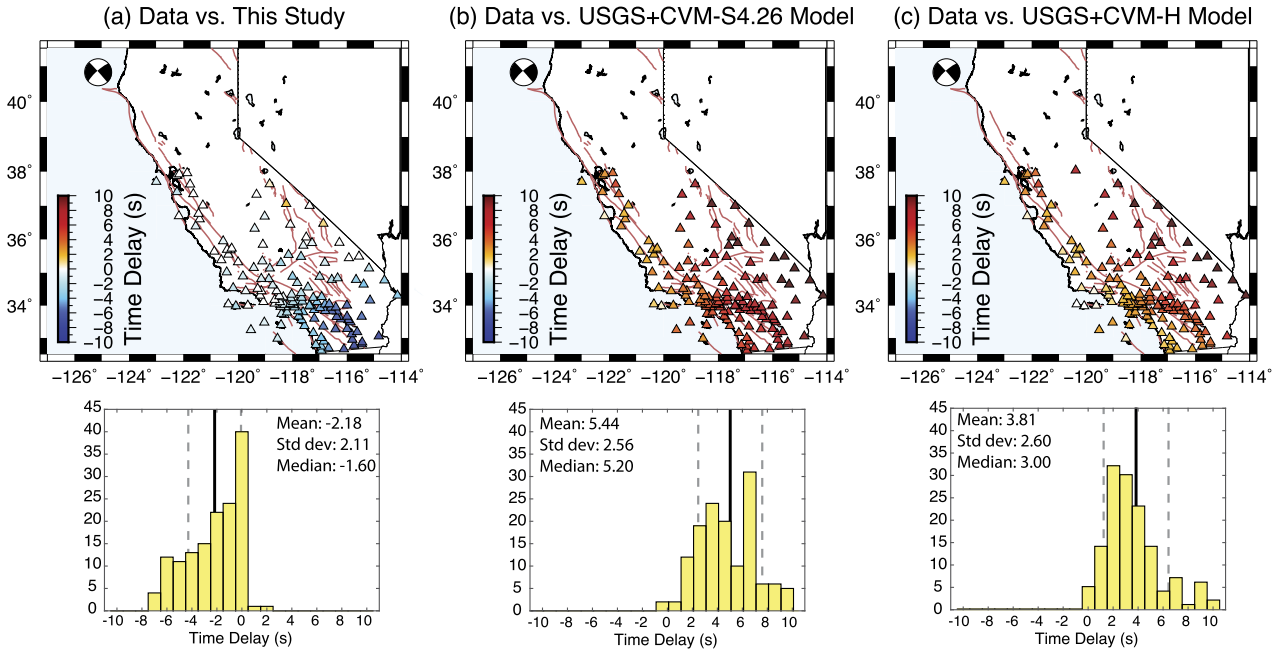

Fig. 9. Maps show the time delay between the recorded long period SH waves from the 2014 Mendocino event, and the synthetics from (a) our preferred model, (b) USGS Bay Area and CVM-S4.26 Southern California model and (c) USGS Bay Area and CVM-Harvard Southern California model. Cooler color indicates the recorded seismograms arrive earlier than the synthetics. Histograms below the map show the distribution of the time delays for each model comparison. (For interpretation of the colors in this figure, the reader is referred to the web version of this article.)

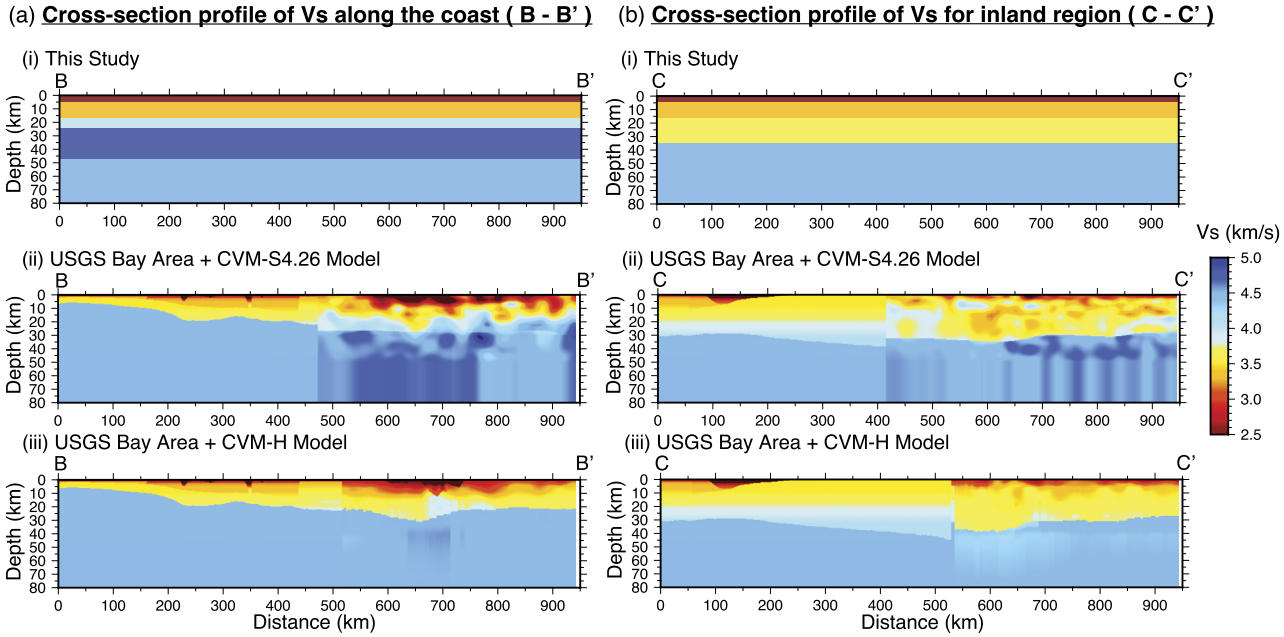

Fig. 10. Cross-section profiles of shear wave (V_S) structure along Profile B–B′ (coast) and Profile C–C′ (inland) for three 3D velocity models. The profile locations are indicated in Fig. 7.

form boundary does not necessarily follow the surface trace of SAF, but rather it is a zone up to 80 km wide, notably centered west of the SAF in southern California, and has a trend straighter and closer to the plate motion vector than the SAF.

Likewise, our model supports such a significant lateral variation in lithospheric strength or EET with a strong lid west of the plate boundary and a relatively thick, low velocity crust east of the plate boundary. A similar idea of lateral contrast in lithospheric properties is proposed in Ford et al. (2014) through a Sp receiver function study as they observe a change in character of lithosphere–asthenosphere boundary across the plate boundary. In addition, the transform boundary in our simple model, marked by the growth of the lid structure, roughly follows along the local strike of SAF except in Southern California when it moves westward by ∼100 km, which is in agreement with the position of the transform boundary proposed by Platt and Becker (2010). The transform boundary may be characterized as the juxtaposition of the strong Pacific plate due to the seismic lid, with the weak, ductile North American plate, where the lower crust–upper mantle structure beneath the Californian margin controls the strain rate observed in California. This plate boundary structure becomes even more complex in the southernmost portion of southern California

(Imperial Valley) where the crust is quite thin due to the northward impingement of the East Pacific Rise into the North American plate. To more fully explore the consistency of our model with the strain-rate asymmetry and long-term plate deformation in California, additional quantitative analyses are needed which is beyond the scope of the current work.

The velocity contrast in our model bears resemblance to the slab window formed due to the migration of Mendocino Triple Junction during the evolution of the plate boundary (Furlong and Schwartz, 2004). Based on our model, the lithospheric thinning, inferred by Zandt and Furlong (1982) and Wang et al. (2013), may have been a prominent state-wide phenomenon along the east side of the plate boundary at the lower crust–upper mantle depth range. Our model focuses at much shallower depth compared to models from seismic tomography (up to 300 km in Wang et al. (2013)) hence it is less meaningful in terms of understanding past subduction processes or imaging fossil slabs. Nonetheless, our model, constructed from direct seismic observation, can provide useful constraints in the development of the next generation state-wide velocity models and informing the regional plate tectonic history.

This study illustrates the potential of using regional waveforms to investigate the laterally varying seismic velocity structure of the lower crust–upper mantle beneath California. Our simplified model, i.e. a fast seismic lid underlying the Pacific plate abutting against a thick crust with relatively low seismic velocities comprising the continental North American plate, does well at reproducing the systematic travel time variations of long period Sn waves observed across central and southern California for events in the Mendocino region. The strong heterogeneity in velocity suggests similar heterogeneity in lithospheric strength, which may modulate the plate deformation in this region.

Acknowledgements

This work is supported by USGS Earthquake Hazards Program award G15AP00029 along with partial support from NSF-Earthscope program, EAR-1358646 and USGS Cooperative Agreement G14AC00109. Constructive reviews provided by Brad Aagaard, Annemarie Baltay, Carl Tape and an anonymous reviewer were very helpful in improving the manuscript. Waveform data for this study were accessed through the Northern California Earthquake Data Center (NCEDC), http://dx.doi.org/10.7932/NCEDC, and Southern California Earthquake Data Center (SCEDC) at Caltech, http://dx.doi.org/10.7909/C3WD3xH1. Maps were created using General Mapping Tools (GMT) software (Wessel et al., 2013).

Appendix A. Supplementary material

Supplementary material related to this article can be found online at http://dx.doi.org/10.1016/j.epsl.2017.02.002.

References

Aagaard, B.T., Graves, R.W., Rodgers, A., Brocher, T.M., Simpson, R.W., Dreger, D., Petersson, N.A., Larsen, S.C., Ma, S., Jachens, R.C., 2010. Ground-motion modeling of Hayward fault scenario earthquakes, part II: simulation of long-period and broadband ground motions. Bull. Seismol. Soc. Am. 100, 2945–2977.

Ammon, C.J., Zandt, G., 1993. Receiver structure beneath the Southern Mojave Block, California. Bull. Seismol. Soc. Am. 83, 737–755.

Anderson, D.L., 1995. Lithosphere, asthenosphere, and perisphere. Rev. Geophys. 33, 125–149.

Brocher, T.M., McCarthy, J., Hart, P.E., Holbrook, W.S., Furlong, K.P., McEvilly, T.V., Hole, J.A., Klemperer, S.L., 1994. Seismic evidence for a lower-crustal detachment beneath San Francisco bay, California. Science 265, 1436–1439.

Chery, J., 2008. Geodetic strain across the San Andreas fault reflects elastic plate thickness variations (rather than fault slip rate). Earth Planet. Sci. Lett. 269, 352–365.

Dreger, D., Romanowicz, B., 1994. Source characteristics of events in the San Francisco Bay region. U.S. Geol. Surv. Open-File Rept. 94-176, 301–309.

Ford, H.A., Fischer, K.M., Lekic, V., 2014. Localized shear in the deep lithosphere beneath the San Andreas fault system. Geology 42, 295–298.

Furlong, K.P., Schwartz, S.Y., 2004. Influence of the Mendocino triple junction on the tectonics of coastal California. Annu. Rev. Earth Planet. Sci. 32, 403–433.

Gaherty, J.B., Kato, M., Jordan, T.H., 1999. Seismological structure of the upper mantle: a regional comparison of seismic layering. Phys. Earth Planet. Inter. 110, 21–41.

Grand, S.P., Helmberger, D.V., 1984. Upper mantle shear structure of North-America. Geophys. J. Int. 76, 399–438.

Graves, R.W., 1996. Simulating seismic wave propagation in 3D elastic media using staggered-grid finite differences. Bull. Seismol. Soc. Am. 86, 1091–1106.

Hadley, D., Kanamori, H., 1977. Seismic structure of the transverse ranges, California. Geol. Soc. Am. Bull. 88, 1469–1478.

Hauksson, E., 2000. Crustal structure and seismicity distribution adjacent to the Pacific and North America plate boundary in southern California. J. Geophys. Res. 105, 13875.

Helmberger, D.V., Song, X.J., Zhu, L., 2001. Crustal complexity from regional waveform tomography: aftershocks of the 1992 Landers earthquake, California. J. Geophys. Res. 106, 609.

Herrmann, R.B., 2013. Computer programs in seismology: an evolving tool for instruction and research. Seismol. Res. Lett. 84, 1081–1088.

Jennings, C.W., 1994. Fault activity map of California and adjacent areas, with locations and ages of recent volcanic eruptions California Department of Conservation, Division of Mines and Geology. Geologic Data Map No. 6.

Ji, C., Tsuboi, S., Komatitsch, D., Tromp, J., 2005. Rayleigh-wave multipathing along the west coast of North America. Bull. Seismol. Soc. Am. 95, 2115–2124.

Kohlstedt, D.L., Evans, B., Mackwell, S.J., 1995. Strength of the lithosphere – constraints imposed by laboratory experiments. J. Geophys. Res., Solid Earth 100, 17587–17602.

Lee, E.-J., Chen, P., Jordan, T.H., Maechling, P.B., Denolle, M.A.M., Beroza, G.C., 2014. Full-3-D tomography for crustal structure in Southern California based on the scattering-integral and the adjoint-wavefield methods. J. Geophys. Res., Solid Earth 119, 6421–6451.

Lekic, V., French, S.W., Fischer, K.M., 2011. Lithospheric thinning beneath rifted regions of Southern California. Science 334, 783–787.

Levander, A., Miller, M.S., 2012. Evolutionary aspects of lithosphere discontinuity structure in the western US. Geochem. Geophys. Geosyst. 13.

Melbourne, T., Helmberger, D., 2001. Mantle control of plate boundary deformation. Geophys. Res. Lett. 28, 4003–4006.

Platt, J.P., Becker, T.W., 2010. Where is the real transform boundary in California? Geochem. Geophys. Geosyst. 11, 1525–2027.

Prindle, K., Tanimoto, T., 2006. Teleseismic surface wave study for S-wave velocity structure under an array: Southern California. Geophys. J. Int. 166, 601–621.

Schmalzle, G., Dixon, T., Malservisi, R., Govers, R., 2006. Strain accumulation across the Carrizo segment of the San Andreas Fault, California: impact of laterally varying crustal properties. J. Geophys. Res. 111.

Shaw, J.H., Plesch, A., Tape, C., Suess, M.P., Jordan, T.H., Ely, G., Hauksson, E., Tromp, J., Tanimoto, T., Graves, R., Olsen, K., Nicholson, C., Maechling, P.J., Rivero, C., Lovely, P., Brankman, C.M., Munster, J., 2015. Unified structural representation of the southern California crust and upper mantle. Earth Planet. Sci. Lett. 415, 1–15.

Song, X.J., Helmberger, D.V., Zhao, L., 1996. Broad-band modelling of regional seismograms: the basin and range crustal structure. Geophys. J. Int. 125, 15–29.

Stein, S., Wysession, M., 2009. An Introduction to Seismology, Earthquakes, and Earth Structure. John Wiley & Sons.

Tan, Y., Helmberger, D.V., 2007. Trans-Pacific upper mantle shear velocity structure. J. Geophys. Res. 112.

Tape, C., Liu, Q., Maggi, A., Tromp, J., 2009. Adjoint tomography of the southern California crust. Science 325, 988–992.

Tape, C., Plesch, A., Shaw, J.H., Gilbert, H., 2012. Estimating a continuous Moho surface for the California unified velocity model. Seismol. Res. Lett. 83, 728–735.

Wang, Y., Forsyth, D.W., Rau, C.J., Carriero, N., Schmandt, B., Gaherty, J.B., Savage, B., 2013. Fossil slabs attached to unsubducted fragments of the Farallon plate. Proc. Natl. Acad. Sci. USA 110, 5342–5346.

Wdowinski, S., Smith-Konter, B., Bock, Y., Sandwell, D., 2007. Diffuse interseismic deformation across the Pacific–North America plate boundary. Geology 35, 311.

Wessel, P., Smith, W.H.F., Scharroo, R., Luis, J., Wobbe, F., 2013. Generic mapping tools: improved version released. Eos, Trans. Am. Geophys. Union 94, 409–410.

Yan, Z., Clayton, R.W., 2007. Regional mapping of the crustal structure in southern California from receiver functions. J. Geophys. Res. 112.

Zandt, G., Furlong, K.P., 1982. Evolution and thickness of the lithosphere beneath coastal California. Geology 10, 376.

Zhao, L.-S., Helmberger, D.V., 1994. Source estimation from broadband regional seismograms. Bull. Seismol. Soc. Am. 84, 91–104.

Zhu, L., Helmberger, D.V., 1996. Advancement in source estimation techniques using broadband regional seismograms. Bull. Seismol. Soc. Am. 86, 1634–1641.

Zhu, L., Kanamori, H., 2000. Moho depth variation in southern California from teleseismic receiver functions. J. Geophys. Res. 105, 2969.

Zhu, L., Rivera, L.A., 2002. A note on the dynamic and static displacements from a point source in multilayered media. Geophys. J. Int. 148, 619–627.